

Quantum variational measurement in the next generation gravitational-wave detectors

F.Ya.Khalili*

Physics Faculty, Moscow State University, Moscow 119992, Russia

(Dated: November 5, 2019)

A relatively simple method of overcoming the Standard Quantum Limit in the next-generation Advanced LIGO gravitational wave detector is considered. It is based on the quantum variational measurement with a single short (a few tens of meters) filter cavity. Estimates show that this method allows to reduce the radiation pressure noise at low frequencies (< 100 Hz) to the level comparable with or smaller than the low-frequency noises of non-quantum origin (mirrors suspension noise, mirrors internal thermal noise, and gravity gradients fluctuations).

I. INTRODUCTION

The sensitivity of the first generation large-scale laser interferometric gravitational wave detectors operating now is extremely high. They can detect mechanical displacement as small as $\sim 10^{-16}$ cm [1]. This sensitivity provides a real chance to detect gravitational waves from astrophysical sources [2, 3]. However, routine observations of gravitational waves require at least one order of magnitude better sensitivity.

This sensitivity improvement is planned for the second generation detectors, in particular, the Advanced LIGO [4, 5, 6, 7]. As a consequence, the Advanced LIGO sensitivity will be close to the Standard Quantum Limit (SQL) [8]. This limitation corresponds to the sensitivity level where the meter measurement noise (the shot noise in the optical interferometric position meters case) becomes equal to the meter back action noise (*i.e.* the radiation pressure fluctuations). The first noise is inversely proportional to the optical power and the second one is directly proportional to it.

Several methods of overcoming the SQL have been proposed. One of the most promising is the *quantum variational measurement* [9, 10, 11, 12, 13]. It uses correlation between the measurement noise and back-action noise, which allows, in principle, to remove the back-action noise component from the meter output. Frequency-independent correlation can be introduced in the optical position meters relatively easy by using homodyne detector with properly adjusted local oscillator phase. However, in this case the back-action suppression is possible in narrow frequency band only.

The method of creating the frequency-dependent noise correlation in large-scale laser interferometric gravitational wave detectors was proposed and analyzed in detail in the article [14]. It is based on the use of additional *filter cavities* which introduce frequency-dependent phase shift into the reflected light. These cavities can be placed before the main interferometer (so-called *modified input optics* case) as well as after it (*modified output optics*). In the former case a squeezed quantum state have to be used. In the latter one, it is not necessary

*Electronic address: farid@hbar.phys.msu.ru

but desirable because allows to decrease the required optical power. The comprehensive analysis of this technology application to the signal recycled topology, planned for the Advanced LIGO and used in the operating now smaller GEO-600 gravitational wave detector [15], was performed in the articles [16, 17].

The main technical problem of this method arises due to the requirement that the filter cavities bandwidths should be of the same order of magnitude as the gravitational-wave signal frequency $\Omega \sim 10^3 \text{ s}^{-1}$. Therefore, the filter cavities quality factors have to be as high as $\omega_p/\Omega \sim 10^{12}$, where $\omega_p \sim 10^{15} \text{ s}^{-1}$ is the laser pumping frequency. Therefore, long filter cavities with very high-reflectivity mirrors should be used. Filter cavities with the same length as the main interferometer cavities (4 Km), placed in the same vacuum chamber side-by-side with the latter ones, were considered in the article [14]. This topology allows, in principle, to obtain sensitivity significantly better than the SQL and probably will be used in the third (post Advanced LIGO) generation of the laser gravitational-wave detectors (see brief discussion on the technical issues of this topology in paper [18]).

In the current article the topology based on the same principle but less ambitious and more simple in implementation is considered. It contains only one relatively short filter cavity with length comparable to the Advanced LIGO auxiliary mode-cleaner cavities: a few tens of meters. We suppose here that the main interferometer parameters values are close to those planned for the Advanced LIGO. In particular, we suppose that:

- the optical power circulating in the interferometer arms is equal to the power necessary to reach the SQL, $W = W_{\text{SQL}} \approx 840 \text{ kW}$;
- the interferometer is tuned in resonance and thus the “optical springs” technology [19, 20] is not used;
- no quantum squeezed states are used

(see the brief discussion on the last two items in the Conclusion). It should be noted that the case of short (30 meters long) cavities was considered in paper [17]. However, the authors of this paper followed the original optimization procedure of [14] which does not provide very good results for such short cavities. Here we propose another optimization method more suitable for short filter cavities with relatively high optical losses.

It follows from the planned Advanced LIGO noise budget that the only frequency range where it is possible to increase the sensitivity without the increase of circulating power and/or use of squeezed quantum states, and without reducing the mirrors internal noise, is the low-frequency area $\Omega/2\pi \lesssim 100 \text{ Hz}$, where the sensitivity is limited by the radiation-pressure noise. It is this area that is considered in this article.

In Sec. II, the measurement scheme is discussed and the the main equations used in this paper are introduced. In Sec. III a new “soft” variant of variational measurement optimization is considered. In Sec. IV, the achievable sensitivity is estimated. The main notations and parameters values used in this paper are listed in Table I.

II. THE SCHEME

The scheme considered in this article is shown in Fig. 1(left). Basically, it is signal/power recycled Advanced LIGO interferometer topology with additional filter cavity in the output port. Variant with ring filter cavity is shown. An ordinary Fabry-Perot cavity can be also

Quantity	Value for estimates	Description
Ω		Gravitational-wave frequency
c	3×10^8 m/s	Speed of light
ω_p	1.77×10^{15} s $^{-1}$	Optical pumping frequency
M	40 kg	Mirror mass
L	4 km	Interferometer arms length
γ		Interferometer half-bandwidth
A^2	10^{-5}	Interferometer optical losses per bounce
$\mathcal{A} = \frac{cA^2}{4L\gamma}$	3×10^{-4}	Interferometer effective loss factor
W	840 kW	Power circulating in each of the arms
$J = \frac{8\omega_p W}{McL}$	$(2\pi \times 100$ s $^{-1})^3$	
L_f		Filter cavity length
T_f^2		Filter cavity input mirror transmittance
A_f^2	10^{-5}	Filter cavity losses per bounce
γ_f		\approx Filter cavity half-bandwidth
δ_f		Filter cavity detuning

TABLE I: Main notations used in this paper.

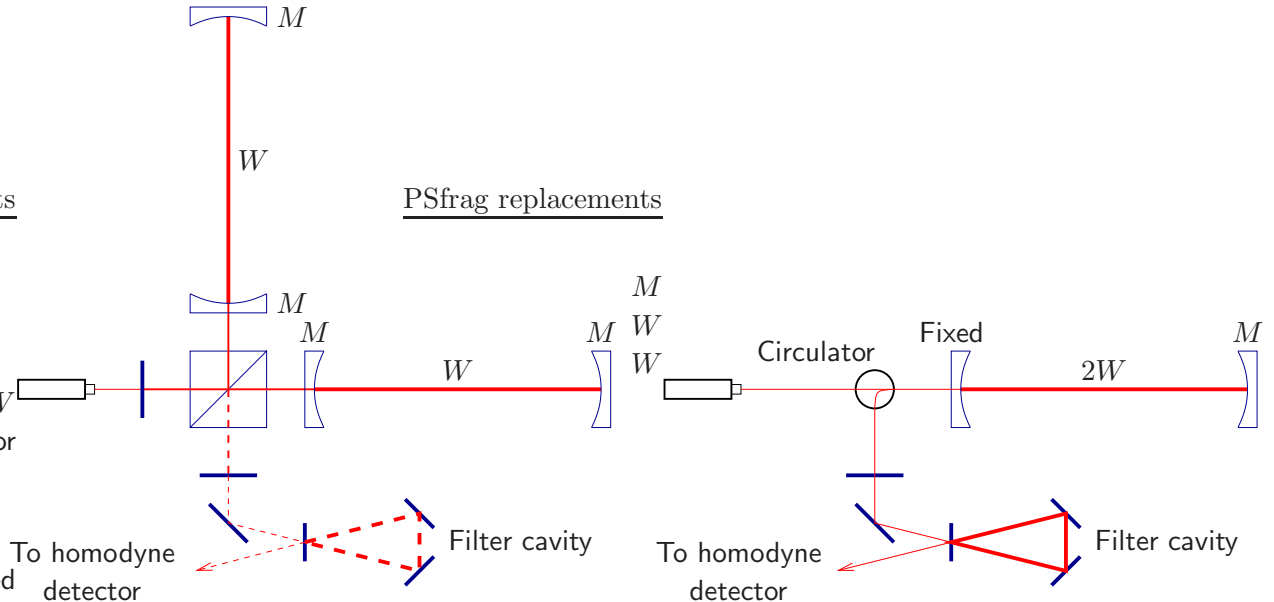


FIG. 1: Left: the signal/power recycled Advanced LIGO interferometer with additional filter cavity; right: simplified equivalent scheme.

used; however, some circulator is necessary in this case to separate the filter cavity output beam from the input one. On the other hand, only one end mirror is required instead of two in the latter case, which allows to decrease the cavity internal losses.

It was shown in article [21], that the Advanced LIGO topology can be mapped to a simple Fabry-Perot cavity based optical position meter, with fixed input mirror and movable end

one. The end mirror mass should be equal to the mass of each of four Advanced LIGO mirrors, the cavity length should be equal to the Advanced LIGO arms length, and the circulating optical power should be twice as high as the circulating power in each of the Advanced LIGO arms [see Fig.1(right)]. It is this equivalent scheme that will be used for calculations below.

The sum quantum noise of the scheme in Fig.1 has been calculated in paper [18]. If the interferometer is tuned in resonance, then it can be presented as follows:

$$\xi^2(\Omega) \equiv \frac{S^h(\Omega)}{S_{\text{SQL}}^h(\Omega)} = \frac{\Omega^2(\Omega^2 + \gamma^2)[1 + \mathcal{A}_\Sigma(\Omega)]}{4J\gamma \cos^2 \phi_\Sigma(\Omega)} - \tan \phi_\Sigma(\Omega) + \frac{J\gamma}{\Omega^2(\Omega^2 + \gamma^2)}, \quad (1)$$

where $S^h(\Omega)$ is spectral density of the equivalent strain noise,

$$S_{\text{SQL}}^h(\Omega) = \frac{8\hbar}{ML^2\Omega^2} \quad (2)$$

is the spectral density corresponding to the SQL,

$$\phi_\Sigma(\Omega) = \phi + \phi_f(\Omega), \quad (3)$$

ϕ is the local oscillator phase,

$$\phi_f(\Omega) = \arctan \frac{2\gamma_f \delta_f}{\Omega^2 + \gamma_f^2 - \delta_f^2} \quad (4)$$

is the phase shift in filter cavity,

$$\mathcal{A}_\Sigma = \mathcal{A} + \mathcal{A}_f(\Omega) \quad (5)$$

is the sum effective losses factor,

$$\mathcal{A}_f(\Omega) = \frac{cA_f^2}{L_f} \frac{\gamma_f(\Omega^2 + \gamma_f^2 + \delta_f^2)}{\Omega^4 + 2(\gamma_f^2 - \delta_f^2)\Omega^2 + (\gamma_f^2 + \delta_f^2)^2} \quad (6)$$

is the effective losses factor of filter cavity.

Function (1) will be compared below with the one corresponding to the ideal ($\mathcal{A}_\Sigma = 0$) SQL-limited ($\phi_\Sigma = 0$) interferometer:

$$\xi_{\text{SQL}}^2(\Omega) = \frac{\Omega^2(\Omega^2 + \gamma^2)}{4J\gamma} + \frac{J\gamma}{\Omega^2(\Omega^2 + \gamma^2)}. \quad (7)$$

It is convenient to separate in Eq. (1) terms of different origin:

$$\xi^2(\Omega) = \xi_{\text{SN}}^2(\Omega) + \xi_{\text{res}}^2(\Omega) + \xi_{\text{loss}}^2(\Omega), \quad (8)$$

where

$$\xi_{\text{SN}}^2(\Omega) = \frac{\Omega^2(\Omega^2 + \gamma^2)[1 + \mathcal{A}_\Sigma(\Omega)]}{4J\gamma} \quad (9a)$$

is the component created by the shot noise,

$$\xi_{\text{res}}^2(\Omega) = \xi_{\text{SN}}^2(\Omega) \left[\tan \phi_\Sigma(\Omega) - \frac{1}{2\xi_{\text{SN}}^2(\Omega)} \right]^2 \quad (9b)$$

is the residual part of the back-action noise, and

$$\xi_{\text{loss}}^2(\Omega) = \frac{\mathcal{A}_\Sigma(\Omega)}{4\xi_{\text{SN}}^2(\Omega)} \quad (9c)$$

is the component created by optical losses.

III. SOFT VARIATIONAL MEASUREMENT

The standard variational measurement approach is to eliminate completely the back-action noise by setting

$$\tan \phi_{\Sigma}(\Omega) - \frac{1}{2\xi_{\text{SN}}^2(\Omega)} \equiv 0. \quad (10)$$

With only one filter cavity, this equality can not be fulfilled exactly for all frequencies Ω . Moreover, in the presence of optical losses, two filter cavities are also insufficient for it. On the other hand, in case of short filter cavity, the exact fulfillment of condition (10) does not allow to obtain arbitrary high sensitivity, anyway, due to the losses term (9c).

At the same time, the term (9b) can be reduced significantly and made smaller than the other two terms in Eq. (8) even when only one filter cavity is used. Condition (10) should be fulfilled approximately in this case:

$$\tan \phi_{\Sigma}(\Omega) - \frac{1}{2\xi_{\text{SN}}^2(\Omega)} \approx 0. \quad (11)$$

It is evident that this *soft variational measurement* optimization can be performed in many different ways, depending on the desirable shape of the resulting noise spectral density. However, in the particular case considered here, taking into account the constraints listed in the Introduction, the parameters choice is rather unique.

Let us start with the high-frequency area, $\Omega \gg \gamma$, where

$$\xi_{\text{loss}}(\Omega) \rightarrow 0, \quad \xi_{\text{res}}^2(\Omega) \approx \xi_{\text{SN}}^2(\Omega) \tan^2 \phi, \quad (12)$$

and

$$\xi^2(\Omega) \approx \frac{\xi_{\text{SN}}^2(\Omega)}{\cos^2 \phi}. \quad (13)$$

Therefore, in order to keep this noise as small as possible, there should be

$$\phi = 0. \quad (14)$$

It should be noted, that in ordinary meters (*i.e.*, without variational measurement), using $\phi \neq 0$, it is possible to obtain some sensitivity gain at low ($\Omega < \gamma$) or medium ($\Omega \sim \gamma$) frequencies at the cost of increased high-frequency noise. With variational measurement this trade-off is possible too, but in this case the gain is small compared to the gain provided by variational measurement itself. Therefore, the only case of $\phi = 0$ is considered here.

At low frequencies ξ_{res}^2 is approximately equal to

$$\xi_{\text{res}}^2(\Omega) \Big|_{\Omega \ll \gamma} \approx \frac{\Omega \gamma [1 + \mathcal{A}_{\Sigma}(0)]}{J} \left\{ \frac{\gamma_f \delta_f}{\Omega^2 + \gamma_f^2 - \delta_f^2} - \frac{J}{\Omega^2 \gamma [1 + \mathcal{A}_{\Sigma}(0)]} \right\}^2. \quad (15)$$

This expression is equal to zero, if

$$\gamma_f = \delta_f, \quad \gamma_f \delta_f = \frac{J}{\gamma [1 + \mathcal{A}_{\Sigma}(0)]}. \quad (16)$$

The last equations specify the filter cavity parameters:

$$\gamma_f = \delta_f = \frac{1}{1 + \mathcal{A}} \left[\sqrt{\frac{(1 + \mathcal{A})J}{\gamma} + \left(\frac{cA_f^2}{4L_f} \right)^2} - \frac{cA_f^2}{4L_f} \right]. \quad (17)$$

The only free parameter remaining is the interferometer half-bandwidth γ . Typically, it is supposed for wide band configurations like the one considered here, that $\gamma \approx J^{1/3}$. However, asymptotic values of $\xi(\Omega)$ at both low and high frequencies decrease with γ increase. At medium frequencies $\Omega \sim J^{1/3}$, the optimal value of γ which provides minimum of $\xi(\Omega)$ exists. It depends on Ω , but this dependence is rather weak. Therefore, the value of

$$\gamma_{\text{opt}} \approx 1.7J^{1/3}, \quad (18)$$

which provides the minimum of $\xi(\Omega)$ at $\Omega = J^{1/3}$, will be used in the estimates below.

The explicit expressions for the noise components can be obtained by substituting Eqs. (17) into Eqs. (9). However, the resulting expressions are too cumbersome. Below we present the approximate formulae corresponding to the lossless case for ξ_{SN} , and ξ_{res} , and the expression for ξ_{loss} , where only the first non-vanishing in loss factors A^2, A_f^2 terms are kept:

$$\xi_{\text{SN}}^2(\Omega) \approx \frac{\Omega^2(\Omega^2 + \gamma^2)}{4J\gamma}, \quad (19a)$$

$$\xi_{\text{res}}^2(\Omega) \approx \frac{J\Omega^2}{\gamma^3(\Omega^2 + \gamma^2)}, \quad (19b)$$

$$\xi_{\text{loss}}^2(\Omega) \approx \frac{J\gamma}{\Omega^2(\Omega^2 + \gamma^2)} \left[\mathcal{A} + \frac{cA_f^2}{L_f} \sqrt{\frac{J}{\gamma}} \frac{\Omega^2 + 2J/\gamma}{\Omega^4 + (2J/\gamma)^2} \right]. \quad (19c)$$

IV. THE SENSITIVITY

At low frequencies, quantum noise of the considered scheme depends on the *specific losses factors* A^2/L and A_f^2/L_f of the main interferometer and the filter cavity, correspondingly. If mirrors produced at the same technological level, are used in both cases, $A^2 \approx A_f^2$, then filter cavity losses play the main role, because $L \gg L_f$. In the estimates below, the following values for filter cavity losses will be used: $5 \times 10^{-7} \text{ m}^{-1}$ (for example, 20 m filter cavity with $A_f^2 = 10^{-5}$) and 10^{-7} m^{-1} .

In order to demonstrate the back action noise suppression level in the optimization procedure considered above, the noise components $\xi_{\text{loss}}^2(\Omega)$, $\xi_{\text{res}}^2(\Omega)$, and $\xi_{\text{SN}}^2(\Omega)$ are plotted separately in Fig. 2, for $A_f^2/L_f = 5 \times 10^{-7} \text{ m}^{-1}$. It follows from this plot, that the residual back action noise is indeed much smaller than at least one of two other noise components.

In Fig. 3, the sum noise factor $\xi(\Omega)$ is plotted for two values of A_f^2/L_f mentioned above, together with low frequency asymptotics for $\xi_{\text{loss}}(\Omega)$ and with the corresponding function (7) for the SQL-limited meter. These plots show that, at high frequencies, the sum noise is still shot-noise limited while, at low frequencies, there is a significant sensitivity gain. It is limited by optical losses only, mostly by filter cavity losses.

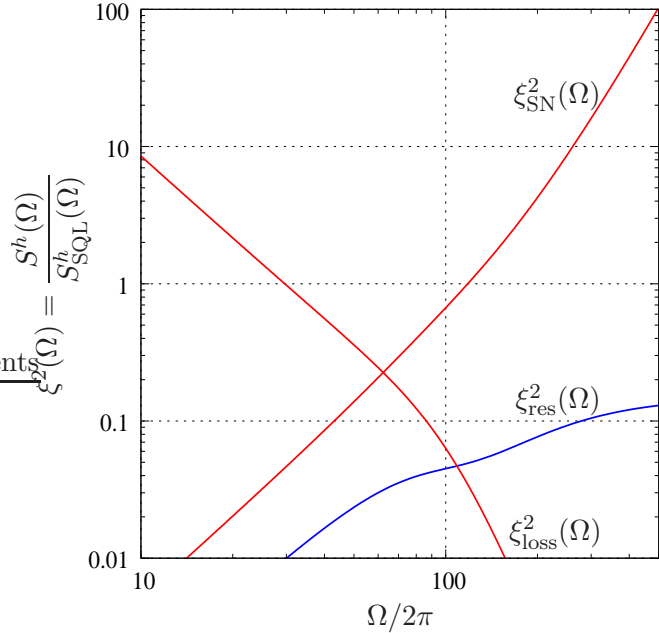


FIG. 2: Plots of the noise components $\xi_{\text{loss}}^2(\Omega)$, $\xi_{\text{res}}^2(\Omega)$, and $\xi_{\text{SN}}^2(\Omega)$. Filter cavity losses are equal to $A_f^2/L_f = 5 \times 10^{-7} \text{ m}^{-1}$.

The explicit expression for this sensitivity gain can be obtained using Eqs. (7) and (19c):

$$\left. \frac{\xi_{\text{loss}}(\Omega)}{\xi_{\text{SQL}}(\Omega)} \right|_{\Omega \rightarrow 0} \approx \sqrt{\frac{cA_f^2}{2L_f}} \sqrt{\frac{\gamma}{J}} \approx 0.17 \sqrt{\frac{A_f^2/L_f}{10^{-7}}}. \quad (20)$$

Therefore, for realistic filter cavity parameters values, the low-frequency sensitivity 3 \div 5 times better than the SQL can be obtained.

In Fig. 4, square root of the equivalent strain noise $\sqrt{S^h(\Omega)}$ (long dashes) is plotted on top of the standard Advanced LIGO noise budget picture [7]. This plot allows to compare directly quantum noise of the scheme considered here with the main noises of non-quantum origin predicted for the Advanced LIGO, and also with the equivalent strain noise of the ordinary wide-band SQL-limited meter (short dashes). It should be noted that the direct comparison with the quantum noise curve of picture [7] is incorrect. This curve involves another technique of overcoming the SQL, based on the optical rigidity, which is used to increase the detection range for neutron star-neutron star inspiral events. As a result, the quantum noise is suppressed at medium frequencies (~ 100 Hz), while rises at higher frequencies.

V. CONCLUSION

It follows from the estimates made in this paper that using variational measurement with single relatively short filter cavity, it is possible to reduce the back action noise in the Advanced LIGO interferometer to the level comparable to or smaller than the low-frequency noises of non-quantum origin: mirrors suspension noise, mirrors internal thermal noise, and gravity gradients fluctuations. The minimal reasonable filter cavity length for the best

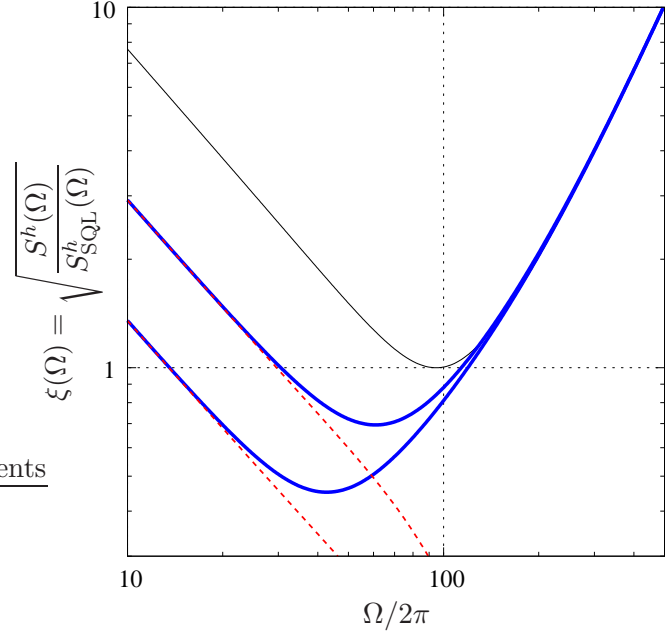


FIG. 3: Plots of: $\xi_{\text{SQL}}(\Omega)$ (thin solid), $\xi(\Omega)$ (thick solid), and $\xi_{\text{loss}}(\Omega)$ (dashed). For $\xi(\Omega)$ and $\xi_{\text{loss}}(\Omega)$, upper lines correspond to $A_f^2/L_f = 5 \times 10^{-7} \text{ m}^{-1}$ and lower ones — to $A_f^2/L_f = 1 \times 10^{-7} \text{ m}^{-1}$.

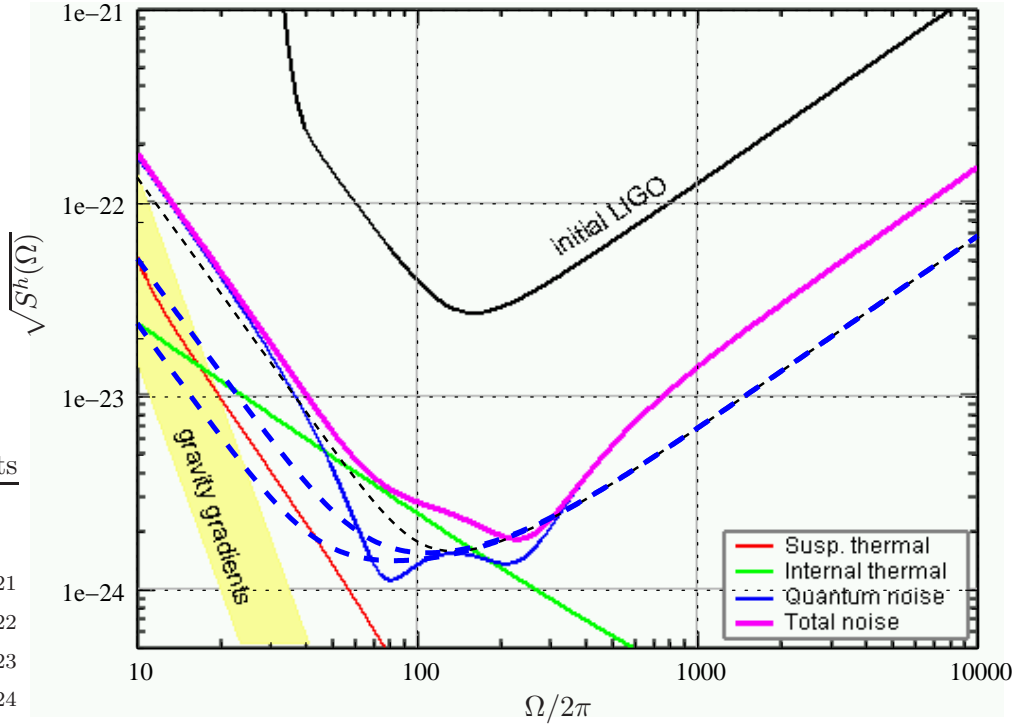


FIG. 4: Square root of the sum noise spectral density $\sqrt{S^h(\Omega)}$ plotted on top of the standard Advanced LIGO noise budget picture [7] (solid), for $A_f^2/L_f = 5 \times 10^{-7} \text{ m}^{-1}$ (long dashes, upper) and $A_f^2/L_f = 1 \times 10^{-7} \text{ m}^{-1}$ (long dashes, lower). Plot for the wide-band SQL $\sqrt{S_{\text{SQL}}^h(\Omega)}$ (short dashes) is provided for the comparison.

mirrors available (with losses per bounce $\sim 10^{-5}$) is about $10 \div 20$ m. In this case, $2 \div 3$ -fold increase of the Advanced LIGO sensitivity at low frequencies ($10 \div 50$ Hz) is feasible. Better mirrors, with losses per bounce $\lesssim 5 \times 10^{-6}$ and/or longer filter cavity would be able to virtually remove the back-action noise from the Advanced LIGO noise budget.

It is evident, that the scheme considered here can be combined with other methods, which also allows to increase the interferometric gravitational wave detectors sensitivity without significant modifications of the topology and without the increase of optical power. In particular, using the the optical rigidity [19, 20, 22], it is possible to reshape the noise spectral dependence, extending the low frequency sensitivity gain to the medium frequencies range.

Another promising option is the squeezed vacuum injection into the interferometer dark port [23]. It allows to decrease the shot noise at the cost of increased radiation pressure noise (for the same value of the mean optical power). The radiation pressure noise, in turn, can be reduced at low frequencies by using variational measurement of the type considered here. In paper [24] the method of generation of squeezed states with frequency-dependent *amplitude* of squeezing, which could provide an additional suppression of the radiation-pressure noise, was proposed. Taking into account the recent achievements in preparation of squeezed quantum states at low frequencies ($10 \div 1000$ Hz) [25, 26], it possible to hope that this combination could provide the sensitivity gain of $\sim 2 \div 3$ within the entire Advanced LIGO frequency band.

Acknowledgments

This work was supported by the NSF and Caltech grant PHY-0353775 and by Russian government grant NSh-5178.2006.2.

The author is grateful to V.Braginsky, Y.Chen, S.Danilishin, N.Mavalvala, K.Strain, and S.Vyatchanin for stimulating discussions and useful remarks. The author is grateful also to Y.Chen for the remark about the “slack” low-frequency area in the Advanced LIGO noise budget which stimulated this paper writing.

- [1] Jay Marx, Status of Some Aspects of LIGO, 2006, LIGO Document G060101-00-M (www.ligo.caltech.edu/docs/G/G060101-00.pdf).
- [2] A.Abramovici *et al*, Science **256**, 325 (1992).
- [3] K.S.Thorne, in *Proceedings of the Snowmass 95 Summer Study on Particle and Nuclear Astrophysics and Cosmology*, edited by E.W.Kolb and R.Peccei, page 398, World Scientific, Singapore, 1995, gr-qc/9506085.
- [4] K.S.Thorne, The scientific case for mature ligo interferometers, 2000, LIGO document P000024-00-R (www.ligo.caltech.edu/docs/P/P000024-00.pdf).
- [5] E.Gustafson, D.Shoemaker, K.A.Strain and R.Weiss, LSC White paper on detector research and development, 1999, LIGO Document T990080-00-D (www.ligo.caltech.edu/docs/T/T990080-00.pdf).
- [6] P.Fritschel, Second generation instruments for the Laser Interferometer Gravitational-wave Observatory (LIGO), in *Gravitational Wave Detection, Proc. SPIE*, volume 4856-39, page 282, 2002.

- [7] <http://www.ligo.caltech.edu/advLIGO>.
- [8] V.B.Braginsky, Sov. Phys. JETP **26**, 831 (1968).
- [9] E.G.Unruh, in *Quantum Optics, Experimental Gravitation, and Measurement Theory*, edited by P.Meystre and M.O.Scully, page 647, 1982.
- [10] F.Ya.Khalili, Doklady Akademii Nauk **294**, 602 (1987).
- [11] M.T.Jaekel and S.Reynaud, Europhysics Letters **13**, 301 (1990).
- [12] A.F.Pace, M.J.Collect and D.F.Walls, Physical Review A **47**, 3173 (1993).
- [13] S.P.Vyatchanin and A.B.Matsko, Sov. Phys. JETP **83**, 690 (1996).
- [14] H.J.Kimble, Yu.Levin, A.B.Matsko, K.S.Thorne and S.P.Vyatchanin, Physical Review D **65**, 022002 (2002).
- [15] B.Willke *et al.*, Classical and Quantum Gravity **19**, 1377 (2002).
- [16] Jan Harms, Yanbei Chen, Simon Chelkovski, Alexander Franzen, Hennig Walbruch, Karsten Danzmann, and Roman Schnabel, Physical Review D **68**, 042001 (2003).
- [17] A.Buonanno, Y.Chen, Physical Review D **69**, 102004 (2004).
- [18] F.Ya.Khalili, arXiv:gr-qc/0607028 (2006).
- [19] A.Buonanno, Y.Chen, Physical Review D **64**, 042006 (2001).
- [20] A.Buonanno, Y.Chen, Physical Review D **65**, 042001 (2002).
- [21] A.Buonanno, Y.Chen, Physical Review D **67**, 062002 (2003).
- [22] V.B.Braginsky, F.Ya.Khalili, Physics Letters A **257**, 241 (1999).
- [23] C.M.Caves, Physical Review D **23**, 1693 (1981).
- [24] Thomas Corbitt, Nergis Mavalvala, and Stan Whitcomb, Physical Review D **70**, 022002 (2004).
- [25] K.McKenzie, N.Grosse, W.P.Bowen, S.E.Whitcomb, M.B.Gray, D.E.McClelland, P.K.Lam, Physical Review Letters **95**, 211102 (2005).
- [26] H.Vahlbruch, S.Chelkowski, B.Hage, A.Franzen, K.Danzmann, and R.Schnabel, Physical Review Letters **97**, 011101 (2006).